

# A Flow Representation for EFD/CFD Integrated Visualization

**Kaori Hattanda<sup>1)</sup> Takayuki Itoh<sup>1)</sup>**

**Shigeya Watanabe<sup>2)</sup> Shigeru Kuchi-ishi<sup>2)</sup> Kanako Yasue<sup>2)</sup>**

1) Department of Information Sciences, Ochanomizu University

2) Japan Aerospace Exploration Agency

{kaori-h, itot}@itolab.is.ocha.ac.jp, {shigeyaw, shigeruk}@chofu.jaxa.jp, yasue.kanako@jaxa.jp

## Abstract

EFD (Experimental Flow Dynamics) and CFD (Computational Flow Dynamics) are two major research fields for analysis of flow phenomena. We focus on development of EFD/CFD integrated visualization which aims comparison and analysis of results of EFD and CFD. We especially have attempted to visualize the pressure and airflow around airplanes obtained as results of EFD and CFD, and have already presented a visualization of air pressure on the surfaces of airplanes. As the second step of our work, this paper presents a visualization of airflow around the airplanes obtained as results of EFD and CFD. Our representation is effective for the comparison of vortices as well as vector fields between results of EFD and CFD.

## 1. Introduction

Experimental Fluid Dynamics (EFD) and Computational Fluid Dynamics(CFD) are two major research fields for analysis and of flow phenomena. EFD technologies measure directions and velocities of airflows by using special equipments such as wind tunnels. EFD has relatively longer history and therefore many researchers feel EFD is more reliable; however, it has several limitations including costs and schedules. CFD is relatively easier to have more variety of results; however, we need to verify the results of CFD by comparing with corresponding results of EFD. Integration of both techniques is more effective to complement the drawbacks, and bring better knowledge from each technique.

We have been focusing on integrated visualization of EFD and CFD for the comparison of both results and supplement of their drawbacks. As the first step of the work, we have presented an integrated visualization technique of scalar fields of EFD and CFD[1], especially for air pressure on the surfaces of airplanes. This paper presents our development on integrated visualization of vector fields of EFD and CFD, especially airflow around airplanes as results of EFD and CFD, as the second step of our work. This paper demonstrates the effectiveness by applying the airflow around an airplane.

## 2. Related Work

This section introduces related studies on EFD/CFD integration, EFD/CFD integrated visualization, and vortex-oriented flow visualization.

### 2.1 EFD/CFD Integration

There are few well-known systems on the integration of EFD and CFD in the field of aerospace. ViDI (Virtual Diagnostics Interface System)[2] by NASA Langley laboratory is a typical EFD/CFD integrated system. It compares real-time EFD results and pre-computed CFD results and quickly visualizes their difference. Also, JAXA (Japan Aerospace Exploration Agency) is developing a concurrent EFD/CFD integration system so called Digital/Analog hybrid wind-tunnel[3]. In such systems, visualization is a very important technical component to help users compare and understand the results of EFD and CFD.

### 2.2 EFD/CFD Integrated Visualization

We have presented an EFD/CFD integrated visualization technique and applied to air pressure on the surfaces of airplanes [1]. It firstly integrates mesh structure between EFD and CFD, and then visualizes their scalar fields and differences between them calculated on the integrated mesh. The technique also overlays sharp-gradient lines of EFD and CFD. The sharp-gradient lines are often observed around critical regions such as shockwaves around airplanes, and therefore comparison of the sharp-gradient lines between EFD and CFD is an important process to verify these results each other.

### 2.3 Vortex-oriented Flow Visualization

Critical points such as vortices are always important for flow analysis, and therefore they are often emphatically drawn in flow visualization. Our technique features integrated visualization of vortices between EFD and CFD. It applies a critical point extraction method[4], which extracts positions that the velocity of a vector fields is zero as critical points. The

critical points can be theoretically divided into several types: vortices, saddles, and so on.

### 3. Implementation Detail

Our implementation of the presented technique consists of two major components: data integration and cortex extraction. Figure 1 shows a dataset we visualized in this work. Air pressure on the surface of the airplane is represented by the color of the surface. Air flow behind the airplane is represented by a set of arrows on a plane. The left side of the figure is the result of CFD, and the right side of the figure is the result of EFD.

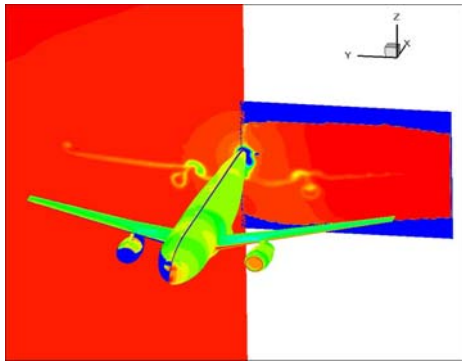


Figure 1. Example of visualization of air pressure and airflow as the results of EFD and CFD.

#### 3.1 Data Unification

We suppose that both EFD and CFD datasets form mesh structure. Generally we cannot expect that mesh structures of EFD and CFD datasets are similar. It is necessary to unify the mesh structure so that we can calculate the differences of velocity between EFD and CFD. Our implementation calculates velocities of results of CFD at the cell-vertices of EFD, because basically we would like to trust the results of EFD and therefore fit the results of CFD onto the results of EFD. The following is the processing flow of integration of results of CFD onto the mesh structure of EFD, where Figure 2 shows the correspondence between mesh structures of EFD and CFD:

1. Project the position of a cell-vertex  $Ve$  in the mesh structure of EFD at the position  $Ve'$  in the mesh structure of CFD.
2. Specify the cell  $Cc$  which encloses  $Ve'$ .
3. Calculate the velocity value at  $Ve'$  by interpolating velocity values at the cell-vertices of  $Cc$ .
4. Repeat 1. to 3. for all the cell-vertices of the mesh structure of EFD.

Figure 3 shows the interpolation scheme applied to the velocity at a point inside a triangular cell. The scheme firstly divides the quadrilateral cell into two triangles and specify the one of them which encloses the position  $Ve'$ . It then calculates the areas of three triangles,  $S_{12}$ ,  $S_{13}$ , and  $S_{23}$ . Here, the triangle which encloses  $Ve'$  is divided to generate the three triangles, by connecting each of its cell-vertices and  $Ve'$ . Also, it calculates  $v_{12}$ ,  $v_{13}$ , and  $v_{23}$ , average

velocity values of the three triangles. Finally, the scheme calculates the velocity  $v$  at  $Ve'$ , as the average of the velocities at the cell-vertices while weighting by the areas of three triangles.

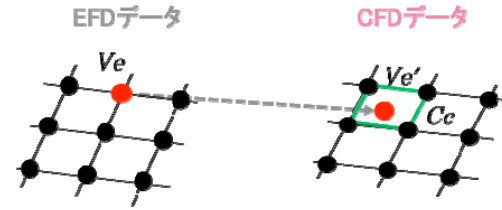


Figure 2. Integration of results of CFD onto the mesh structure of EFD.

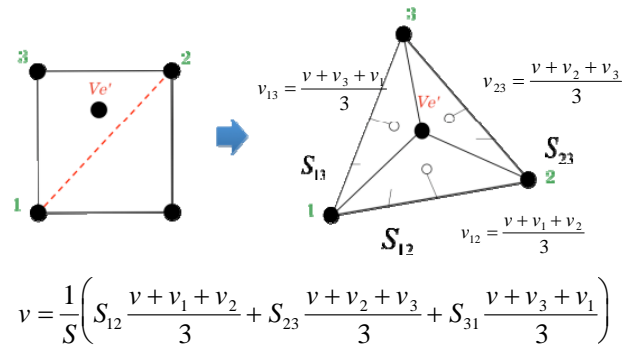


Figure 3. Velocity interpolation.

Our implementation calculates the differences of velocities between EFD and CFD after the unification process. It finally represents the distribution of velocities (or their differences) by colors.

#### 3.2 Vortex Extraction

Vortex observation is important in flow visualization, because airflow around vortices is often unstable, and therefore it may cause damages or energy inefficiency. Visualization of vortices behind airplanes assists understanding of forces to airplanes due to the airflow. Figure 4 shows an example of vortex behind the wing tip of an airplane.

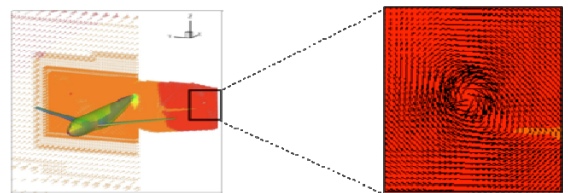


Figure 4. Example of vortex behind an airplane.

Velocity is zero at the center of a vortex. In other words, vortices can be discovered by extracting the position where the velocities are zero, and then dividing the positions according to the numeric features of vector fields around them. Our implementation applies a technique [3] which extracts zero-velocity positions to generate meaningful streamlines for flow visualization. Supposing that a vector field is given on an XY-plane, the processing flow for extracting zero-velocity positions is as follows:

1. Determine if a zero-velocity position exists in a cell  $Cc$ .
2. Calculate the position where the velocity is zero, if it is

determined that the position exists in  $Cc$ .

3. Determine if the zero-velocity position is the center of vortex or not.
4. Repeat 1. to 3. for all of cells.

Our implementation determines the existence of zero-velocity positions as follows. Let a cell  $Cc$  triangular, positions of its three cell-vertices  $(y_0, z_0)$ ,  $(y_1, z_1)$  and  $(y_2, z_2)$ , and velocity of a flow at the three cell-vertices  $(v_0, w_0)$ ,  $(v_1, w_1)$  and  $(v_2, w_2)$ . Our implementation calculates the real values  $p$  and  $q$  satisfying the following equation:

$$\begin{pmatrix} 0 \\ 0 \end{pmatrix} = \begin{pmatrix} v_0 \\ w_0 \end{pmatrix} \times p + \begin{pmatrix} v_1 \\ w_1 \end{pmatrix} \times q + \begin{pmatrix} v_2 \\ w_2 \end{pmatrix} \times (1 - p - q)$$

It determines that a zero-velocity position exists in  $Cc$ , if  $p$  and  $q$  satisfies the following equation:

$$0 \leq p, 0 \leq q, 0 \leq 1 - p - q$$

In this case, the zero-velocity position is calculated by the following equation:

$$\begin{pmatrix} y \\ z \end{pmatrix} = \begin{pmatrix} y_0 \\ z_0 \end{pmatrix} \times p + \begin{pmatrix} y_1 \\ z_1 \end{pmatrix} \times q + \begin{pmatrix} y_2 \\ z_2 \end{pmatrix} \times (1 - p - q)$$

The zero-velocity positions can be divided into centers of vortices and others. Here, the Jacobian matrix of the airflow in  $Cc$  is calculated by the following equation:

$$J_v = \begin{bmatrix} \frac{\partial v}{\partial y} & \frac{\partial v}{\partial z} \\ \frac{\partial w}{\partial y} & \frac{\partial w}{\partial z} \end{bmatrix} = \begin{bmatrix} \frac{\partial v}{\partial y} & \frac{\partial v}{\partial z} \\ \frac{\partial w}{\partial y} & \frac{\partial w}{\partial z} \end{bmatrix} \times \begin{bmatrix} \frac{\partial y}{\partial v} & \frac{\partial y}{\partial w} \\ \frac{\partial z}{\partial v} & \frac{\partial z}{\partial w} \end{bmatrix}$$

$$= \begin{bmatrix} y_0 - y_2 & y_1 - y_2 \\ z_0 - z_2 & z_1 - z_2 \end{bmatrix}^T \times \begin{bmatrix} V_0 - V_2 & V_1 - V_2 \\ Z_0 - Z_2 & Z_1 - Z_2 \end{bmatrix}$$

The position is a center of vortex if the eigenvalue of  $J_v$  is complex and its real part is not zero.

Our implementation displays vorticity by colors as well as positions of vortices. Vorticity is a metric for degree of rotation of a vortex, where its absolute value denotes the strength of the vortex, and its sign denotes the direction of the flow. It calculates the vorticity on the YZ-plane by the following equation:

$$rotV = \nabla \times \mathbf{V} = \frac{\partial w}{\partial y} - \frac{\partial v}{\partial z}$$

## 4. Example

This section shows examples of visualization by our implementation. We applied an airplane model DLR-F6, supposing Much number as 0.75, and angle of attack as 0.19. Flow fields measured behind the airplane is recorded on an YZ-plane. The EFD result is drawn at the left side, while the CFD result is drawn in the right side in the following examples.

## 4.1 Vortex Extraction

Figure 5 shows an example of vortex extraction result, where centers of vortices in the EFD result are indicated as green squares in the left side, and ones in the CFD result are indicated in the right side. Several vortices were observed as the result of turbulent flow behind the engines. Vortices are also observed around the wing tips.

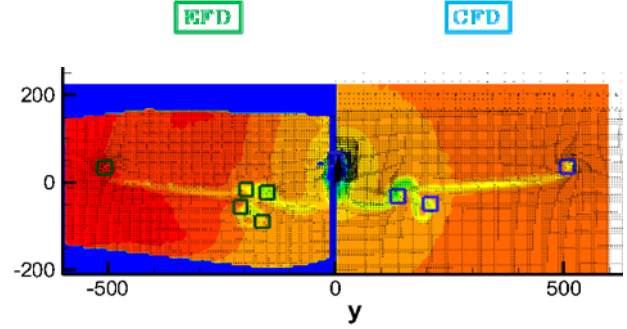


Figure 5. Centers of vortices displayed as green/blue squares.

We projected the center of a vortex behind the wing tips from EFD to CFD. Also, we projected the one from CFD to EFD. Figure 6 shows the result, where two squares in the zoomed regions denote the centers of vortices of EFD and CFD. The distance between the two centers was about 0.001 times of the width of an airplane. It denotes that the measurement and simulation results around the wing tips were very reliable.

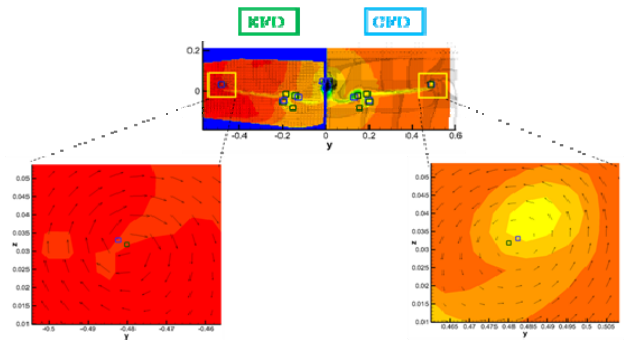


Figure 6. Projection of centers of vortices between EFD and CFD.

## 4.2 Vorticity

Figure 7 shows a result of vorticity calculation, where blue portions denote clockwise rotation, and red portions denote counterclockwise rotation. Figure 7(Upper) shows only the distribution of vorticity, and Figure 7(Lower) shows the distribution of vorticity and flow direction.

Figure 8 shows a zoom up of vorticity distribution around wing tips, where the result of CFD is horizontally reversed. In this figure red portions have nearly zero values of vorticity, and non-red regions have clockwise rotations. This visualization denotes that vorticity in the EFD result was much stronger than vorticity in the CFD result, and therefore the EFD result demonstrated much stronger resistance to the body of the

airplane than the CFD result.

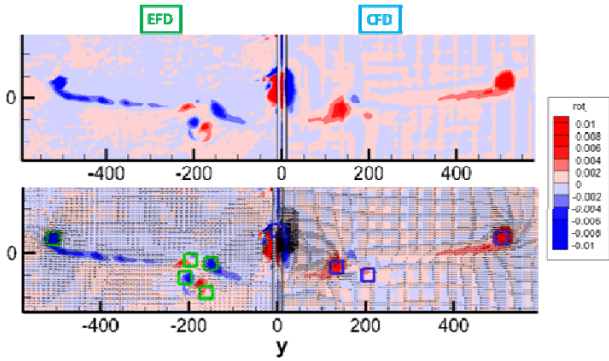


Figure 7. Vorticity.

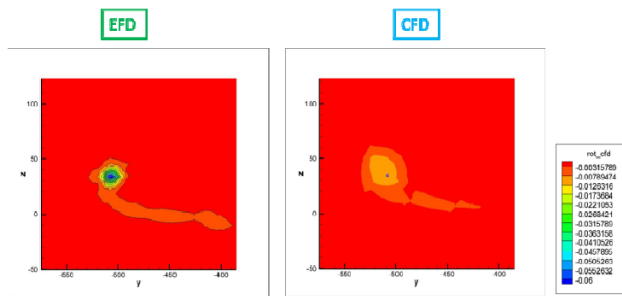


Figure 8. Vorticity behind wing tips.

### 4.3 Difference

Figure 9 shows the difference of the YZ-element of velocity between EFD and CFD. Here, red portions denote that velocity of EFD is larger, while blue portions denote that velocity of CFD is larger.

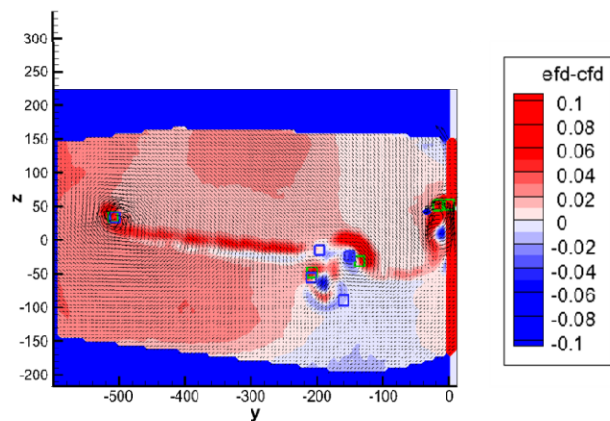


Figure 9. Difference of velocity between EFD and CFD.

Figure 10 shows a zoom up around wing tips. The result denotes that the velocity fields of EFD and CFD contain 7.8% error in maximum, while normalizing the velocity values so that the predefined standard velocity is 1.

This kind of visualization is useful for error analysis of EFD and CFD. EFD may cause errors due to errors and aging of models, skill of engineers, and uncertainty of experiment

environments. CFD also may cause errors due to various computational errors, and incompleteness of discrete analysis models and formulations. Our visualization system will contribute to understand the errors between EFD and CFD and improve them.

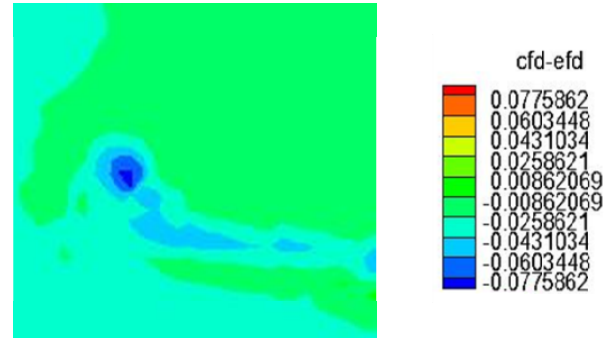


Figure 10. A zoom up of the difference of velocity between EFD and CFD around wing tips.

## 5. Conclusion

This paper presented a flow representation running on our EFD/CFD integrated visualization system. As future issues, we would like to develop more sophisticated error visualization schemes considering gaps between centers of vortices. Also, we would like to develop a scheme to effectively visualize distribution of errors. We will apply more variety of airplane models and prove the effectiveness of our system.

## References

- [1] S. Kasamatsu, T. Itoh, S. Watanabe, S. Kuchi-ishi, K. Yasue, A Study on Visualization for EFD/CFD Integration, IEEE Pacific Visualization 2011, Poster Session, 2011.
- [2] R. J. Schwarts, G. A. Fleming, Virtual Diagnostics Interface: Real Time, Comparison of Experimental Data and CFD Predictions for a NASA Ares I-Like Vehicle, International Congress on Instrumentation in Aerospace Simulation Facilities 07, R56, 2007.
- [3] S. Watanabe, S. Kuchi-ishi, et al., A Trial towards EFD/CFD Integration - JAXA Digital/Analog Hybrid Wind Tunnel -, JAXA-SP-08-009, 2008.
- [4] K. Nakakita, K. Mitsuno, M. Kurita, S. Watanabe, K. Yamamoto, J. Mukai, CFD Code validation Using Pressure-Sensitive Paint Measurement, JAXA-SP-04-012, 2004.
- [5] K. Koyamada, T. Itoh, Seed Specification for Displaying a Streamline in an Irregular Volume, Engineering with Computers, 14, 73-80, 1998.